**Atmospheric
Chemistry
and Physics
Discussions**

# Photochemical modeling of glyoxal at a rural site: observations and analysis from BEARPEX 2007

A. J. Huisman[1,*], J. R. Hottle[1,**], M. M. Galloway[1], J. P. DiGangi[1], K. L. Coens[1], W. S. Choi[2,***], I. C. Faloona[2], J. B. Gilman[3], W. C. Kuster[3], J. de Gouw[3], N. C. Bouvier-Brown[4,****], A. H. Goldstein[4], B. W. LaFranchi[5,*****], R. C. Cohen[5], G. M. Wolfe[6,******], J. A. Thornton[6], K. S. Docherty[7,*******], D. K. Farmer[7,********], M. J. Cubison[7], J. L. Jimenez[7], J. Mao[8,*********], W. H. Brune[8], and F. N. Keutsch[1]

[1]Dept. of Chemistry, University of Wisconsin-Madison, Madison, Wisconsin, USA
[2]Dept. of Land, Air, and Water Resources, Univ. of California-Davis, Davis, California, USA
[3]NOAA Earth System Research Laboratory and Cooperative Institute for Research in Environmental Sciences, University of Colorado, Boulder, CO, USA
[4]Dept. of Environmental Science, Policy, and Management, University of California, Berkeley, CA, USA
[5]Dept. of Chemistry, University of California, Berkeley, CA, USA
[6]Dept. of Chemistry, University of Washington, Seattle, WA, USA

Discussion Paper | Discussion Paper | Discussion Paper | Discussion Paper

**ACPD**

11, 13655–13691, 2011

**Modeling of glyoxal at a rural site**

A. J. Huisman et al.

Title Page

Abstract | Introduction

Conclusions | References

Tables | Figures

◀ | ▶

◄ | ►

Back | Close

Full Screen / Esc

Printer-friendly Version

Interactive Discussion

[7] CIRES and Dept. of Chemistry and Biochemistry, Univ. of Colorado, Boulder, CO, USA

[8] Dept. of Meteorology, Pennsylvania State University, University Park, Pennsylvania, USA

[*] now at: Institute for Atmospheric and Climate Science, ETH Zurich, Zurich, Switzerland

[**] now at: Air Force Office of Scientific Research–Physics and Electronics Directorate, Arlington, VA, USA

[***] now at: Dept. of Atmospheric and Oceanic Sciences, University of California, Los Angeles, Los Angeles, California, USA

[****] now at: Chemisty & Biochemistry Department, Loyola Marymount University, Los Angeles, California, USA

[*****] now at: Physical and Life Sciences Directorate, Lawrence Livermore National Laboratory, Livermore, California, USA

[******] now at: Dept. of Chemistry, University of Wisconsin-Madison, Madison, Wisconsin, USA

[*******] now at: Alion Science and Technology, EPA Office of Research and Development, Research Triangle Park, North Carolina , USA

[********] now at: CIRES and Dept. of Chemistry and Biochemistry, Univ. of Colorado, Boulder, Colorado, USA

[*********] now at: Program in Atmospheric and Oceanic Sciences, Princeton University, Princeton, New Jersey, USA

Title Page

Abstract | Introduction

Conclusions | References

Tables | Figures

◄ | ►

◄ | ►

Back | Close

Full Screen / Esc

Printer-friendly Version

Interactive Discussion

## Abstract

We present ∼ one month of high time-resolution, direct, in situ measurements of gas-phase glyoxal acquired during the BEARPEX 2007 field campaign. The research site, located on a ponderosa pine plantation in the Sierra Nevada mountains, is strongly influenced by biogenic volatile organic compounds (BVOCs); thus this data adds to the few existing measurements of glyoxal in BVOC-dominated areas. The short lifetime of glyoxal of ∼ 1 h, the fact that glyoxal mixing ratios are much higher during high temperature periods, and the results of a photochemical model demonstrate that glyoxal is strongly influenced by BVOC precursors during high temperature periods.

A zero-dimensional box model using near-explicit chemistry from the Leeds Master Chemical Mechanism v3.1 is used to investigate the processes controlling glyoxal chemistry during BEARPEX 2007. The model shows that MBO is the most important glyoxal precursor (∼ 67%), followed by isoprene (∼ 26%) and methylchavicol (∼ 6%), a precursor previously not commonly considered for glyoxal production. The model calculates a noon lifetime for glyoxal of ∼ 0.9 h, making glyoxal well suited as a local tracer of VOC oxidation in a forested rural environment; however, the modeled glyoxal mixing ratios over-predict measured glyoxal by a factor 2 to 5. Although several parameters, such as an approximation for advection and increased glyoxal loss to aerosol can improve the model measurement discrepancy, reduction in OH is by far the most effective. Reducing OH to half the measured values, which is suggested by preliminary OH measurements using a different technique, decreases the glyoxal over-prediction from a factor of 2.4 to 1.1, as well as the overprediction of $HO_2$ from a factor of 1.64 to 1.14.

## 1 Introduction

Ozone ($O_3$) and aerosols influence climate (Intergovernmental Panel on Climate Change, 2007) and have a direct impact on human health (Bates, 1993; Jakab et al.,

A. J. Huisman et al.

1995) and the biosphere (Karnosky et al., 1996; Percy et al., 2002). It is well established that the formation of $O_3$ and secondary organic aerosol (SOA), which is an important component of ambient aerosol (Zhang et al., 2007), are both directly tied to the gas-phase oxidation of volatile organic compounds (VOCs), in particular in the VOC-$HO_x$-$NO_x$ catalytic cycle ($HO_x \equiv OH + HO_2$, $NO_x \equiv NO + NO_2$) (Kroll and Seinfeld, 2008; Wood et al., 2010; Herndon et al., 2008). Substantial challenges remain, however, in modeling SOA (de Gouw et al., 2005; Volkamer et al., 2006; Goldstein and Galbally, 2007; Carlton et al., 2009; Hallquist et al., 2009) and $O_3$ away from urban centers (e.g., Trainer et al., 1987; Plummer et al., 1996). The challenges for $O_3$ are especially pronounced in rural, forested areas with high biogenic VOC emissions, e.g., terpenes, isoprene, and 2-methyl-3-buten-2-ol (MBO), which together constitute the majority of global non-methane VOC emissions (Guenther et al., 2000). The failure of models in rural vegetated regions, where BVOC and aldehyde reactivity dominates (Steiner et al., 2008), indicates that more attention needs to be paid to primary emissions of oxygenated VOC and the secondary production of oxygenates, of which $\alpha$-dicarbonyls are a subset.

Glyoxal, the smallest ($\alpha$-)dicarbonyl, has a lifetime of only a few hours with respect to photolysis and reaction with OH. Thus, glyoxal can be viewed as a local tracer of VOC oxidation chemistry, which is advantageous for comparisons between models and measurements. According to commonly used mechanisms available in the literature, such as the National Center for Atmospheric Research (NCAR) Master Mechanism, Leeds Master Chemical Mechanism (MCM), and the Mainz Isoprene Mechanism 2 (Madronich and Calvert, 1990; Bloss et al., 2005a,b; Taraborrelli et al., 2009) daytime glyoxal production from BVOCs proceeds largely via reaction of OH, while reaction with ozone contributes relatively little, making glyoxal a promising tracer of OH driven BVOC oxidation. Furthermore, these mechanisms treat glyoxal solely as a higher generation oxidation product of isoprene, MBO and terpenes. All stages of VOC oxidation can contribute to $O_3$ formation, and, for example for isoprene, more than one oxidation step is required to reduce the volatility of products to the extent that partitioning-driven SOA

formation is expected (e.g., Claeys et al., 2004; Edney et al., 2005; Paulot et al., 2009). Thus, glyoxal measurements in rural, forested regions can provide a local tracer of VOC oxidation chemistry, and may be used to test our understanding of higher generation oxidation processes.

5    In addition to the challenges of modeling ozone in forested areas dominated by BVOCs, there recently has been much focus on the often large discrepancies between measured and modeled OH radical concentrations in areas dominated by BVOCs, especially isoprene (Tan et al., 2001; Thornton et al., 2002; Whalley et al., 2011; Ren et al., 2008; Lelieveld et al., 2008; Hofzumahaus et al., 2009; Peeters et al., 2009;
10  Paulot et al., 2009; Peeters and Muller, 2010; Archibald et al., 2010; Stavrakou et al., 2010; da Silva, 2010). Models typically underpredict OH, sometimes by up to an order of magnitude (Lelieveld et al., 2008), relative to observations. A model of atmosphere-forest exchange for the measurement site of the work described here under-predicts OH by a factor of six (Wolfe et al., 2011). As OH radicals are the major oxidizing
15  species in the troposphere this disagreement has large implications for the ability of models to accurately reproduce BVOC oxidation and resulting $O_3$ and SOA formation. A recent intercomparison of the different techniques employed for measuring ambient OH showed slopes in the linear regressions of the daytime measurements of different instruments of 1.01–1.13 for experiments in the SAPHIR chamber and 1.06–1.69 for
20  ambient measurements (Schlosser et al., 2009). This demonstrates that OH continues to prove difficult to measure under all conditions. Clearly, BVOC oxidation and hence production of BVOC oxidation products (OVOCs) depends critically on oxidant concentrations, with OH being of central importance. Thus, using OVOCs as tracers of BVOC oxidation can provide insight into how rapidly BVOC oxidation is occurring, and, if the
25  OVOCs are produced primarily via reaction of OH with BVOCs, their formation will in turn reflect ambient OH concentrations.

In addition to its use as tracer of VOC oxidation chemistry, glyoxal also is of current interest due to its potential direct contribution to SOA formation (Carlton et al., 2007; Volkamer et al., 2007; Corrigan et al., 2008; Nozière et al., 2008; Galloway et al., 2009;

Shapiro et al., 2009; Tan et al., 2009). In models of SOA formation that include glyoxal, it is often a substantial contributor (Carlton et al., 2007; Volkamer et al., 2007; Fu et al., 2008; Ervens and Volkamer, 2010). It is thus important to validate glyoxal concentrations and chemistry in models by comparison with field-measurements. As model studies show that oxidation of BVOCs contributes the majority of glyoxal on a global scale (Fu et al., 2008; Myriokefalitakis et al., 2008; Stavrakou et al., 2009) a comparison with glyoxal measurements for biogenic regions is particularly important.

The site of the Biosphere Effects on AeRosols and Photochemistry EXperiment (BEARPEX) 2007 field campaign, near Blodgett Forest Research Station (BFRS) in the Sierra Nevada, California, is located in a region influenced by high BVOC emissions, in particular of MBO and isoprene as well as terpenes (Lamanna and Goldstein, 1999; Holzinger et al., 2005; Bouvier-Brown et al., 2009) with regular and well characterized meteorology. There have been a number of studies detailing the BVOCs observed at the site (Lamanna and Goldstein, 1999; Holzinger et al., 2005; Bouvier-Brown et al., 2009) making the location ideal for a detailed study of BVOC oxidation.

In this paper we present the first fast (< 1 min), high sensitivity, direct in situ measurements of glyoxal, taken using the Madison Laser-Induced Phosphorescence (MAD-LIP) Instrument (Huisman et al., 2008). We present a description of this new type of data-set for glyoxal, which provides a new point of intercomparison for models in a region dominated by BVOCs. We also present an analysis that investigates the factors influencing glyoxal concentrations at the site and employ glyoxal as a local tracer of VOC oxidation chemistry at the site, in particular with respect to oxidant levels and the sensitivity of model glyoxal concentrations to OH.

Title Page

Abstract | Introduction

Conclusions | References

Tables | Figures

◄ | ►

◄ | ►

Back | Close

Full Screen / Esc

## 2 Measurements site and methods

### 2.1 Site description

Glyoxal mixing ratios were measured during the BEARPEX 2007 campaign at a research site located on a ponderosa pine plantation in the Sierra Nevada mountains, $\sim 80$ km east of Sacramento, CA (38°53′42.9″ N, 120°37′57.9″ W). The site, on Sierra Pacific Industries land, is at an elevation of 1315 m and is near the Blodgett Forest Research Station (BFRS) and has been described in detail previously (Goldstein et al., 2000). It experiences a Mediterranean climate which is typically hot and dry during the summer before transitioning to a cool, wet period starting in September. During the summer, daytime wind is consistently out of the west to southwest while nighttime wind is easterly to northeasterly. The cycling of polluted air from the Central Valley that arrives in late afternoon and clean air from upslope at night leads to regular diurnal patterns in many trace gases (e.g., Lamanna and Goldstein, 1999; Dillon et al., 2002; Murphy et al., 2007; Wolfe et al., 2009).

### 2.2 Madison LIP instrument

Glyoxal data were collected using the Madison LIP Instrument, which has been described in detail elsewhere (Huisman et al., 2008). Briefly, gas phase glyoxal was detected via laser-induced phosphorescence and gated photon counting using a white-type multipass cell. The inherent spectral and temporal resolution of the phosphorescence signal allowed a limit of detection ($3\sigma$) of 18 ppt$_\mathrm{v}$ in 1 min during the BEARPEX 2007 deployment. For the BEARPEX 2007 deployment, the tower portion of the Madison LIP Instrument was initially situated near the south tower, which was 10 m south of the main scaffold tower, on which all measurements to which we compare our data were made except meteorology. The inlet consisted of either 7.6 m or 1 m of 1/2 in OD PTFE tube with no filters of any kind. Field tests showed no discernible inlet effects with respect to length of inlet (cf. Huisman et al., 2008) and more recent tests have

provided additional evidence that the length and material of inlet have negligible effect on the glyoxal signal. While the instrument was near the tower, it used an inlet (7.6 m 1/2 in PTFE tube) at 3.7 m above ground level (a.g.l.) on the tower, where it remained from 24 August–18 September (day of year, DOY, 236 to DOY 261. After 18 September the instrument was placed on the tower, where it remained until the end of glyoxal measurements on 27 September, DOY 270, with a short (1 m) inlet at 12.0 m a.g.l. Tests carried out in the field show that the data from 3.7 m and 12 m a.g.l. are comparable during the daytime, though not necessarily identical (Huisman et al., 2008).

## 2.3 Other measurement techniques

A suite of measurements was available for BEARPEX 2007, including meteorological parameters, such as wind speed and direction, air temperature, humidity, and ozone concentration. Volatile organic compounds where measured using two gas chromatographs with quadrupole mass spectrometers (GC-MS). Speciated acyl peroxy nitrate (APN) measurements were obtained via a thermal dissociation–chemical ionization mass spectrometer. Laser-induced fluorescence instrumentation was used for measurements of OH, $HO_2$ and $NO_2$. Oxygenated organic aerosol (OOA) and hydrocarbon-like organic aerosol (HOA) were obtained using an Aerodyne high-resolution time-of-flight aerosol mass spectrometer. Aerosol surface area was estimated using a scanning mobility particle sizer and observations of boundary layer height were obtained from temperature, humidity, and wind profiles obtained with a tethersonde during BEARPEX 2007. Details of the instrumentation and methods used to obtain these data can be found in Supplement Sect. 1.1.

Title Page

Abstract | Introduction

Conclusions | References

Tables | Figures

|◄ | ►|

◄ | ►

Back | Close

Full Screen / Esc

Printer-friendly Version

Interactive Discussion

## 3 Observations at BEARPEX 2007

### 3.1 General observations

There is only limited glyoxal data available in rural settings and to our knowledge we present the first such data obtained that has a high time resolution obtained with an instrument utilizing a direct, in situ detection method. The complete dataset for glyoxal is presented in Fig. 1 along with ambient temperature and the biogenic VOCs isoprene and MBO, which were the major precursors of glyoxal at the site. Meteorological conditions at BRFS were dry and hot for the majority of the period for which glyoxal data was collected. An abrupt change in weather occurred around DOY 256 (September 13), after which temperatures were substantially lower. The data were divided into a "hot", "cold" and "intermediate" period as defined in the following: the hot period, DOY 240–246 and 248–256, had an average high and low temperature of $\sim 27$, and $\sim 18\,°C$, respectively. The cold period, DOY 247, 256–257, 261–266, had an average high and low temperature of $\sim 15$, and $\sim 8\,°C$, respectively. No measurements were taken on DOY 258–261. The intermediate period, DOY 267–270, had an average high and low temperature of $\sim 19$, and $\sim 9\,°C$, respectively, closer to the cold than the hot period, but the data set was separated from the cold period because of substantially higher glyoxal mixing ratios. The cause of the higher glyoxal mixing ratios during the intermediate period remains unclear, as the average diurnal temperature and VOC profile of this period resembles that of the cold period. The raw data from the Madison LIP Instrument do not show an offset and instrument data logs indicate normal operation during this period, which followed the first rain falls of the season. The substantial change in temperature from hot to cold period provides a basis for studying the dependence of glyoxal concentrations on biogenic emissions, which are strongly tied to temperature (e.g., Guenther et al., 1991; Schade et al., 2000).

The complete dataset for glyoxal, which spans DOY 236–270, had strong diurnal trends with mean of 43.6 ppt$_v$ and median of 41.2 ppt$_v$ with 95% bounds of the complete set of 4.6 ppt$_v$ to 121.7 ppt$_v$ (see Table 1). The measurement uncertainty was

$\sim$ 20%. A previous measurement at this site by Spaulding et al. (2003) found glyoxal mixing ratios of 6–83 ppt$_v$ during 10 days in August and September 2000, with average mixing ratio $27 \pm 15$ ppt$_v$ and a diurnal profile weaker than that observed here. The previous measurements, although occurring in a different year and with different mean temperatures than those reported here, are still within one standard deviation of our mean observations.

The BEARPEX 2007 campaign was located in a region with high BVOC emissions, in particular the glyoxal precursors isoprene and MBO. Thus a strong influence of BVOCs is expected on glyoxal at the site and comparison of the hot and cold period confirms this (see Fig. 2): there is a large difference between hot and cold period in BVOC concentrations and OVOCs that only form from BVOCs, e.g., isoprene, MBO, MVK. Glyoxal shows a similar, but somewhat smaller difference, whereas the anthropogenic tracer propene shows quite different behavior (see Fig. 2). Similarly, daytime concentrations of toluene at the site are essentially unchanged between the two periods, as are those of benzene and other anthropogenic precursors/tracers. Thus, the measurements qualitatively support that there is a strong biogenic influence on glyoxal at the site, and the results from the photochemical model described in Sect. 4.1 supports this.

The correlation of half-hourly glyoxal measurements to measurements of known glyoxal BVOC precursors and BVOC oxidation products are high, whereas correlations with known anthropogenic glyoxal precursors, such as toluene, benzene and acetylene are lower. During the hot period, the strongest correlation was observed with the BVOC oxidation products MPAN ($R^2 = 0.59$, $n = 362$ points), and MVK ($R^2 = 0.41$, $n = 671$), whereas correlations with anthropogenic tracers were substantially smaller, see Table S1. Hot (and cold) period glyoxal was very poorly correlated ($R^2 < 0.10$) with the total OA and OOA factors as measured by Aerosol Mass Spectrometer (AMS) see Table S1. In addition to the poorer correlations of glyoxal with anthropogenic glyoxal precursors, the concentrations of these precursors were low, so that production rates from the BVOCs are much higher, as discussed in Sect. 4.1.

## 3.2 Deposition

The profile of glyoxal on many nights approximated a simple exponential decay, allowing an inference of the deposition rate by fitting in analogy to the method used by Sumner et al. (2001). Six nights were selected which could be fit well with a single-exponential decay in both glyoxal and $O_3$. The results of these fits are presented in Fig. 3, which also includes information on the slope of measured CO during the fitting period (0.8 to 0.2 d; 19.2 to 4.6 h), on a given night in the color of each point. It seems likely that those points exhibiting the least slope in CO indicate a consistent airmass, a requirement for using the decay to fit deposition. The average correlation coefficient between the inferred deposition rates of glyoxal and $O_3$ within each night is good ($R^2 = 0.68$), in agreement with the results of Sumner et al. (2001) for formaldehyde, but the overall correlation is relatively poor ($R^2 = 0.48$, $n = 6$ nights). Thus there is some degree of variability between the relative deposition rates of both glyoxal and $O_3$ on different nights.

The average of the fitted exponential loss rate in glyoxal was $-2.14 \times 10^{-5} \pm 2.7 \times 10^{-6}\,s^{-1}$, which (assuming a nocturnal boundary layer of 70 m, Choi et al., 2010b) corresponds to a deposition velocity of approximately $0.15\,cm\,s^{-1}$, reasonably consistent with the value of Volkamer et al. (2007) of $0.3\,cm\,s^{-1}$. Equating the observed exponential decay to deposition in this manner assumes that there are no important production or loss processes, except for deposition. The photochemical model described in Sect. 4 showed that a 50% higher deposition velocity was required to reproduce the observed loss rate, as according to the model there was slow nighttime glyoxal production.

## 4 Photochemical box model

We employ a photochemical model based on the reactions and kinetics in the Master Chemical Mechanism (MCM) v. 3.1 (Jenkin et al., 1997; Saunders et al., 2003) for comparison with observations to gain insight into the processes controlling glyoxal

Full Screen / Esc

Printer-friendly Version

Interactive Discussion

concentrations during BEARPEX 2007 and to evaluate the degree to which the MCM can be used to represent glyoxal in this rural setting. The model uses the full MCM chemistry for the following species and their oxidation products: isoprene, MBO, $\alpha$-pinene, $\beta$-pinene, acetylene ($C_2H_2$), benzene, and toluene. In addition to well-known

5 biogenic precursors of glyoxal such as MBO and isoprene, we include methylchavicol, an oxygenated aromatic BVOC which was present in substantial concentrations (mean daily maximum of $\sim 0.3\,ppb_v$, with $\sim 0.6\,ppb_v$ as highest observed mixing ratio) during BEARPEX 2007 (Bouvier-Brown et al., 2009). Oxidation of methylchavicol by OH produces glycolaldehyde (see mechanism, Fig. S3) with a direct yield of 37% (Lee et al.,

10 2006). While methylchavicol does not yield as much glycolaldehyde as MBO, which has a corresponding direct yield of $\sim 65\%$ (Chan et al., 2009), it can produce additional glyoxal via higher-generation oxidation processes involving the aromatic system (see Fig. S3).

  In all cases, the model was driven using half-hourly averaged observations of $O_3$,

15 VOCs , campaign diurnally averaged $NO_2$, and temperature period diurnally averaged OH (cf. Sect. 2 for measurement techniques and Sect. 3.1 definition of temperature periods). Different subsets of precursor VOCs were used to explore their influence and determine the main glyoxal VOC precursors. $HO_2$ and intermediates such as MVK were not driven to follow observations, providing comparisons of model and observa-

20 tions in addition to glyoxal. The model used the MCM in conjunction with standard $HO_x$-$NO_x$ cycling with (a) adjustment of yields and production mechanism of glyoxal from isoprene and glycolaldehyde following Galloway et al. (2011), (b) adjustment of MPAN + OH rate constant following the recommendation of Orlando et al. (2002), (c) inclusion of dry deposition, (d) inclusion of loss of gas phase glyoxal to aerosol based

25 on Volkamer et al. (2007), (e) diurnal dilution factor following Pérez et al. (2009), (f) inclusion of methylchavicol degradation chemistry. Details of the implementation are presented in Supplement Sect. 1.2. The model was allowed to "spin-up" to provide approximate starting concentrations for those species for which no measurements were available by looping over the same one hour period 25 times. After this equilibration,

any species for which measurements were available were again set to match observation.

## 4.1 Base-case box model results

The optimized 0-D MCM-based box model described above was used to simulate BEARPEX 2007 conditions and the diurnally averaged model results for the hot period are shown together with the corresponding glyoxal measurement in Fig. 4. The model predicts the following apportionment of production of glyoxal from precursor VOCs (and their oxidation products) during the hot period: 66.8% MBO, 17.7% higher-generation production from isoprene, 6.3% direct isoprene, 5.5% methylchavicol, and 3.7% other (less than 1% each). The anthropogenic VOCs benzene and toluene, as well as acetylene and the pinenes only contribute to a small degree. Although methylchavicol was a small source, contributing about 6% of glyoxal, it is the third most important precursor VOC. Glycolaldehyde is the most important immediate precursor for glyoxal ($\sim 90\%$), and $\sim 75\%$, $\sim 17\%$, $\sim 6\%$, of glycolaldehyde arise from MBO, isoprene and methylchavicol oxidation, respectively. Altogether, these results corroborate the notion that the majority of hot period glyoxal production during BEARPEX 2007 was biogenic in nature, dominated by production from MBO and isoprene.

According to the model, glyoxal has a short ($\sim 0.9$ h) daytime lifetime. The calculated average loss rate and equivalent lifetime in hours as a function of time of day for glyoxal are displayed in Fig. S5. The nighttime loss rate is dominated by reaction with OH and by deposition (cf. discussion of deposition in Sect. 3.2), while daytime loss rate is driven by photolysis, reaction with OH, and dilution with background air (Pérez et al., 2009), all contributing about equally at noon, and aerosol uptake contributing about half of each of the former. The short lifetime of glyoxal makes it ideally suited as a local tracer of VOC oxidation chemistry.

A striking feature of Fig. 4 is the degree of over-prediction of the model compared to the measurements, which is significantly outside of the measurement uncertainty of 20%. In the following section we describe a sensitivity analysis of the parameters that

Title Page

Abstract | Introduction

Conclusions | References

Tables | Figures

|◄ | ►|

◄ | ►

Back | Close

Full Screen / Esc

Printer-friendly Version

Interactive Discussion

were found to be most effective at influencing this over-prediction using only isoprene and MBO as glyoxal precursors. Using the full set of precursor VOCs, with a resulting 1005 species in the MCM is much more computationally demanding than using only MBO and isoprene (219 species in the MCM). In addition, MBO and isoprene contribute the majority of the over-prediction as they produce ca. 90% of glyoxal.

## 4.2 Model sensitivity analysis

In this section we present an analysis of which model parameters were found to most strongly influence the model over-prediction of glyoxal. The following sinks and sources were investigated but found not to substantially contribute to the over-prediction:

– In order for low $NO_x$ chemistry to lower glyoxal noticeably unphysical rate constants for the $RO_2 + HO_2$ reaction had to be employed. In addition, the model employed here matched low $NO_x$ chamber studies of MBO and isoprene very well (Galloway et al., 2011).

– Decreasing glyoxal concentrations noticeably by increased mixing with background air via "vertical dilution" required unphysical dilution rate constants.

– Increasing the daytime deposition velocity by an order of magnitude from the measured nighttime values in view of the recent work by Karl et al. (2010) had only a marginal ($\sim 10\%$) effect.

– Reducing the glyoxal yield for the reaction of OH with glycolaldehyde clearly reduces glyoxal concentrations, however, a reduction to a yield of 0.045 from the original value of 0.29 was required to achieve agreement with average glyoxal measurements. In addition, the yield in the model was tested with chamber experiments of MBO oxidation, which included glycolaldehyde measurements, following BEARPEX 2007 with no observable change in instrument performance and hence should be optimized for this study. In other words, even if the measured

Full Screen / Esc

Printer-friendly Version

Interactive Discussion

glyoxal concentration is biased by some unknown systematic error, analysis of instrument performance strongly indicates that this should match between the field and chamber studies.

The sensitivity of model glyoxal to three parameters will be discussed in more detail: gas-to-aerosol partitioning, altered OH radical concentration, and a treatment of transport.

### 4.2.1 Gas-to-aerosol partitioning

Loss to aerosol has been proposed as an important sink of glyoxal in Mexico City (Volkamer et al., 2007). However, a number of factors are expected to make aerosol less important as a sink during BEARPEX 2007: the aerosol surface areas are about an order of magnitude lower (average aerosol surface areas of $\sim 100$–$200$ mm$^2$ m$^{-3}$). It has been demonstrated that glyoxal uptake mainly depends on aerosol liquid water content (Volkamer et al., 2009), which is expected to be quite low for the dry conditions at BEARPEX 2007 (average daytime and nighttime relative humidity $24.2 \pm 5.6\%$ and $45.7 \pm 10.1\%$, respectively). These facts imply that aerosol loss was not an important sink term for glyoxal during BEARPEX 2007. Additional insight into the role of aerosol as a sink for glyoxal was obtained by analyzing the difference between measured and modeled glyoxal as a function of observed aerosol surface area in model runs that did not include an aerosol loss term (see Fig. S2). If aerosol loss corresponds to an important sink of glyoxal, model-measurement agreement should degrade at high aerosol surface areas. However, this is not the case, in fact a small opposite trend was observed. As a result an increase in the aerosol sink term may improve the average glyoxal overprediction but does so by overcorrecting during periods with higher aerosol load and hardly affecting the overprediction during periods of low aerosol loads. This finding together with the low relative humidities make it unlikely that aerosol loss is one of the main contributors to the over-prediction. However, if glyoxal can be taken up into aerosol under the dry conditions during BEARPEX 2007, a higher value of $\gamma$ would contribute to improving the average discrepancy between model and measurement.

### 4.2.2 Reduced OH radical concentrations

Another means of reducing model glyoxal concentration is to alter the overall oxidation process via changes to OH radical abundance. The results of a sensitivity analysis demonstrate that glyoxal concentrations are very sensitive to OH levels, and results of a model run in which OH was reduced by a factor of two are presented in Fig. 5. Using half measured OH reduces overprediction of daytime glyoxal, defined as 0.35–0.8 d, or 8:30–19:00 h, from $\sim$ 140% to $\sim$ 10%, a reduction of glyoxal of slightly more than a factor of two. In addition, the reduced OH improved the daytime model over-prediction of $HO_2$ from ($\sim$ 64%) to ($\sim$ 14%). Thus, reducing OH to slow overall photochemistry is very effective at improving model agreement with glyoxal and $HO_2$.

It is worth discussing the merits of this sensitivity analysis, as the implications are important within the context of the disagreements between modeled and measured OH discussed in the introduction. The validity of a factor 2 reduction of the OH concentration in the model compared to the reported measurements appears questionable given the measurement absolute accuracy of 32%, 2$\sigma$. Preliminary results from a recent study by the PSU group during BEARPEX 2009 suggest that the measured daytime OH concentrations at this site could potentially be a factor of 2.5 lower than determined with the traditional measurement method used during BEARPEX 2007 (Brune et al., 2010). The implied lower OH concentration refers to the OH concentration experienced over the lifetime of glyoxal and not necessarily the OH concentration at the measurement site. However, there is no reason to expect the OH concentrations to be substantially different. The results show that reducing OH concentrations is one of the most effective means of reducing the glyoxal and $HO_2$ over-predictions and this adjustment, which is in general agreement with the preliminary findings of Brune et al. (2010), has a larger effect than any of the previously discussed parameters, which at present do not have any other corroboration. LaFranchi et al. (2009) found that calculated steady-state concentrations of APNs were as much as two times measured values for the hot period of BEARPEX 2007, despite the fact that the steady-state model is expected

to work well under these conditions. The authors attributed this to uncertainties in the chemistry of peroxy radicals, noting that a factor of three increase in the reaction rate of acyl peroxy radicals with $RO_2$ greatly improved model-measurement agreement. Reducing OH radical concentrations represents another potential solution, as this would decrease the production rate of acyl peroxy radicals.

### 4.2.3 Truncated-Lagrangian-transport model

Transport of glyoxal was not treated explicitly in the 0-D box model. This shortcoming can affect model glyoxal concentrations differently depending on whether the glyoxal precursors are emitted primarily locally, such as MBO, or primarily upwind of the measurement site, as is the case for isoprene. The 0-D model will overestimate glyoxal production for the former case and underestimate it for the latter: MBO is only emitted in a fairly limited spatial region upwind of the measurement site. Whereas in the box model afternoon air masses have experienced MBO processing all day, in reality they have only experienced MBO emissions with subsequent oxidation to glyoxal for a few hours. Major emissions of isoprene occur at a distance from the measurement site and isoprene has already been substantially processed ($> 50\%$) when it arrives at the site. Using the isoprene concentrations observed at the measurement site will under-predict the amount of oxidation products from isoprene, which can be seen in the MVK (and MACR) data shown in Fig. 6. As the daytime lifetime of glyoxal is $\sim 1\,h$, the lack of inclusion of advection in the model is expected to have a limited effect, as transport of $3\,h$ (the noon transport time from the edge of the MBO-emitting region to the measurement site) will have lost most of the original glyoxal. As the 0-D model predicts too much glyoxal, we investigate what the largest possible reduction in over-prediction as a result of transport could be. In this approach we address the overestimate resulting from the locally emitted MBO and neglect the underestimate resulting from isoprene. This represents an upper-limit of the effect of transport.

Using emission maps from Steiner et al. (2007) and measured wind speeds, we calculate the time that air at BFRS is influenced by MBO, for example $\sim 3\,h$ at midday. We

construct a truncated-Lagrangian model in which the Lagrangian model run is initialized when an air-mass with very low glyoxal and glycolaldehyde concentrations ($1 \times 10^5$ molecule cm$^{-3}$) enters the MBO emitting area. For example: the point at noon was estimated to need 3.12 h of transit time to reach the site from the edge of major MBO emissions, so the model concentration of glycolaldehyde was set very low at 8.88 h during each day of the simulation. In this case, air with little glyoxal and glycolaldehyde enters the box at time = 8.88 h. The air-mass then moves with the measured wind-speeds up to the measurement site, which it reaches at noon, and the final value then represents the noon-time model value at the measurement site. Similar runs are performed for each half hour interval. The emission maps show that MBO emissions are fairly homogeneous throughout this region and thus we use the measured MBO concentrations, the most important glyoxal precursor for the entire transect. Site measurements are also used to constrain the other parameters, such as isoprene. As discussed above this is incorrect for isoprene, which has higher concentrations at the entry to the MBO emitting area than our model assumes, and hence would increase glyoxal concentration.

The effect of transport with this truncated Lagrangian model was tested using isoprene and MBO as precursors, which capture 90% of model glyoxal production in the hot period. The upslope wind-flow lasted from about 0.3 day to 0.8 day (7–19 h) on average; no data points are thus reported outside that time. The resultant set of half-hourly endpoints represent the daytime diurnal profile, with the influence of transport reduced or removed (assuming that air entered the MBO emission region with very low or zero concentration of these species). A dot is shown in Fig. 5, corresponding to the endpoints of each of these model runs. Glycolaldehyde is on average reduced to 86% of the original model level (not shown). This suggests that modeled concentrations of glycolaldehyde are only moderately too high due to the failure of the model to treat transport, and hence the 0-D model is not a bad approximation for modeling glycolaldehyde. As expected, the effect on glyoxal, largely a glycolaldehyde oxidation product, is larger. However, the average reduction to 73% of the original prediction is

not sufficient to bring the model into agreement with measurement. For this reason, we conclude that transport alone is clearly not sufficient to explain the over-prediction in modeled glyoxal. In fact, the effect is likely to be smaller, as glyoxal from isoprene is underestimated.

## 4.3 Discussion

Analysis of the model results showed that the majority of glyoxal was formed by glycolaldehyde, which in turn was produced mainly from MBO, and to a lesser degree from isoprene and methylchavicol, which is in agreement with the fact that the glyoxal yield from MBO is substantially higher than from isoprene. The model included all main known precursors for glyoxal that were measured during BEARPEX 2007 and introduced methylchavicol as an additional one. The model substantially ($\sim$ factor 2.5) over-predicts glyoxal at the measurement site. As MBO contributes $\sim$ 70% of glyoxal, MBO oxidation also has to contribute the majority of the over-prediction. An upper-limit estimate of the effect of transport on MBO processing improved model-measurement disagreement but still had a substantial over-prediction ($\sim$ factor 1.8). The slight improvement is a result of the short lifetime of glyoxal during BEARPEX 2007, which limits the effect of transport and supports the notion that glyoxal is a "local" tracer of VOC oxidation chemistry. The effect of transport is expected to be diminished in the model due to the underestimation of glyoxal from isoprene. It is more likely that transport should increase glyoxal due to advection of precursors such as glycolaldehyde (from isoprene) which has approximately twice the lifetime of glyoxal. Other factors that could reduce the over-prediction are increased aerosol loss and a reduced yield of glyoxal from glycolaldehyde. The latter seems unlikely as the work done by Chan et al. (2009) used the Madison LIP instrument to parameterize glyoxal from glycolaldehyde. Since aerosol formation is proportional to liquid water content, the very dry conditions at BEARPEX eliminate aerosol as a significant sink. By far the most effective means to reduce the model over-prediction is reducing the OH concentration, which in addition is the only one supported by other evidence, i.e. the recent work by Brune et al. (2010). In addition, this is the only parameter that also resulted in a substantial improvement

of modeled $HO_2$ concentrations. The high sensitivity of glyoxal to OH is interesting as one might expect OH levels to have little effect on glyoxal as it participates in both production and destruction of glyoxal. The high sensitivity in the model stems from three details of the underlying chemical mechanism and model: (1) the model is driven with measured BVOC concentrations, not emissions, and hence increased OH results directly in increased glycolaldehyde, (2) glyoxal is largely a higher-generation product of BVOC oxidation and thus increased OH increases production of the precursor glycolaldehyde and how fast it is converted to glyoxal, and (3) reaction with OH is not the dominant glyoxal loss channel. Clearly, a combination of adjustment of different parameters can be employed to further improve the model to measurement disagreement. However, such combinations without reduction in OH are not sufficient to reduce modelled glyoxal while, for example, maintaining the correct shape of the diurnal cycle.

## 5   Conclusions

We present the first high time resolution glyoxal data obtained with a direct, in situ detection method in a rural region dominated by BVOC emissions. Measurements of glyoxal during the BEARPEX 2007 campaign were used to examine the influence of BVOCs on glyoxal production and we conclude that during the hot period glyoxal production was dominated by BVOCs. This is supported by the fact that the site is in a region with much higher BVOC than anthropogenic VOC concentrations during high temperature periods combined with the fact that the daytime lifetime of glyoxal is substantially shorter than the transport time from the edge of this region. This is further supported by comparison between hot and cold period glyoxal concentrations. In addition, a photochemical model shows that most of hot period glyoxal production results from BVOCs, primarily MBO and isoprene with a small contribution from methylchavicol, a species that had not previously been taken into account for glyoxal production.

In contrast to the recent work on formaldehyde by Choi et al. (2010a), no evidence can be found that glyoxal is produced via oxidation of unknown/missing BVOC emissions during the hot period. However, this does not imply that such BVOC emissions

do not exist, as only some BVOCs produce glyoxal, whereas formaldehyde is a much more common oxidation product. In addition, the glyoxal observed during the intermediate period cannot be explained with the VOCs measured at BFRS and hence it could indicate an unknown precursor for glyoxal.

Globally, biogenic sources of glyoxal are predicted to exceed anthropogenic sources, so measurements in rural areas are important and we present the first detailed dataset of its kind. This data is also of interest to comparison with modeling studies of glyoxal despite the limitations of measurements at a single ground site as it presents an analysis of the processes controlling glyoxal concentrations in a biogenically influenced area. Thus, the work contributes to the broader understanding of the tropospheric chemistry of glyoxal.

The results of a photochemical model that was successfully tested using chamber studies of isoprene and MBO oxidation were compared to data taken during BEARPEX 2007 showing a substantial over-prediction despite the reduction of higher-generation yields of glyoxal from isoprene. An attempt to model the influence of MBO chemistry more realistically by making an upper-limit estimate of the effect of transport show that this only contributes to a small degree to the over-prediction as does loss of glyoxal to aerosol. A reduction of OH concentrations was determined to be by far the most effective way to reduce glyoxal model concentrations, and in addition is the only adjustment that has supporting evidence based on the recent work by Brune et al. (2010) and improves model $HO_2$ concentrations. This demonstrates that glyoxal can be a useful local tracer of VOC oxidation chemistry, in particular given its short photochemical lifetime. In addition, we propose that the high sensitivity of glyoxal to OH makes it an especially useful tracer for BVOC oxidation studies aimed at investigating OH-driven chemistry.

**Supplementary material related to this article is available online at: http://www.atmos-chem-phys-discuss.net/11/13655/2011/ acpd-11-13655-2011-supplement.pdf**.

# References

Archibald, A. T., Cooke, M. C., Utembe, S. R., Shallcross, D. E., Derwent, R. G., and Jenkin, M. E.: Impacts of mechanistic changes on HO$_x$ formation and recycling in the oxidation of isoprene, Atmos. Chem. Phys., 10, 8097–8118, doi:10.5194/acp-10-8097-2010, 2010. 13659

Bates, D. V.: Detection of chronic respiratory bronchiolitis in oxidant-exposed populations: analogy to tobacco smoke exposure, Environ. Health Perspect., 101(4), 217, 1993. 13657

Bloss, C., Wagner, V., Bonzanini, A., Jenkin, M. E., Wirtz, K., Martin-Reviejo, M., and Pilling, M. J.: Evaluation of detailed aromatic mechanisms (MCMv3 and MCMv3.1) against environmental chamber data, Atmos. Chem. Phys., 5, 623–639, doi:10.5194/acp-5-623-2005, 2005a. 13658

Bloss, C., Wagner, V., Jenkin, M. E., Volkamer, R., Bloss, W. J., Lee, J. D., Heard, D. E., Wirtz, K., Martin-Reviejo, M., Rea, G., Wenger, J. C., and Pilling, M. J.: Development of a detailed chemical mechanism (MCMv3.1) for the atmospheric oxidation of aromatic hydrocarbons, Atmos. Chem. Phys., 5, 641–664, doi:10.5194/acp-5-641-2005, 2005b. 13658

Bouvier-Brown, N. C., Goldstein, A. H., Worton, D. R., Matross, D. M., Gilman, J. B., Kuster, W. C., Welsh-Bon, D., Warneke, C., de Gouw, J. A., Cahill, T. M., and Holzinger, R.: Methyl chavicol: characterization of its biogenic emission rate, abundance, and oxidation

Title Page

| Abstract | Introduction |
| Conclusions | References |
| Tables | Figures |

⏮   ⏭

◀   ▶

Back   Close

Full Screen / Esc

Printer-friendly Version

Interactive Discussion

products in the atmosphere, Atmos. Chem. Phys., 9, 2061–2074, doi:10.5194/acp-9-2061-2009, 2009. 13660, 13666

Brune, W. H., van Duin, D., Mao, J., and Ren, X.: OH and $HO_2$ Measurements in Blodgett Forest, CA during BEARPEX 2009, American Geophysical Union Fall Meeting 2010, 13–17 December, San Francisco, California, USA, 2010. 13670, 13673, 13675

Carlton, A. G., Turpin, B. J., Altieri, K. E., Seitzinger, S., Reff, A., Lim, H. J., and Ervens, B.: Atmospheric oxalic acid and SOA production from glyoxal: results of aqueous photooxidation experiments, Atmos. Environ., 41, 7588–7602, 2007. 13659, 13660

Carlton, A. G., Wiedinmyer, C., and Kroll, J. H.: A review of Secondary Organic Aerosol (SOA) formation from isoprene, Atmos. Chem. Phys., 9, 4987–5005, doi:10.5194/acp-9-4987-2009, 2009. 13658

Chan, A. W. H., Galloway, M. M., Kwan, A. J., Chhabra, P. S., Keutsch, F. N., Wennberg, P. O., Flagan, R. C., and Seinfeld, J. H.: Photooxidation of 2-methyl-3-buten-2-ol (MBO) as a potential source of secondary organic aerosol, Environ. Sci. Technol., 43, 4647–4652, doi:10.1021/es802560w, 2009. 13666, 13673

Choi, W., Faloona, I. C., Bouvier-Brown, N. C., McKay, M., Goldstein, A. H., Mao, J., Brune, W. H., LaFranchi, B. W., Cohen, R. C., Wolfe, G. M., Thornton, J. A., Sonnenfroh, D. M., and Millet, D. B.: Observations of elevated formaldehyde over a forest canopy suggest missing sources from rapid oxidation of arboreal hydrocarbons, Atmos. Chem. Phys., 10, 8761–8781, doi:10.5194/acp-10-8761-2010, 2010a. 13674

Choi, W., Faloona, I. C., McKay, M., Goldstein, A. H., and Baker, B.: Estimating the atmospheric boundary layer height over sloped, forested terrain from surface spectral analysis during BEARPEX, Atmos. Chem. Phys. Discuss., 10, 25759–25801, doi:10.5194/acpd-10-25759-2010, 2010b. 13665

Claeys, M., Graham, B., Vas, G., Wang, W., Vermeylen, R., Pashynska, V., Cafmeyer, J., Guyon, P., Andreae, M. O., Artaxo, P., and Maenhaut, W.: Formation of secondary organic aerosols through photooxidation of isoprene, Science, 303, 1173–1176, doi:10.1126/science.1092805, 2004. 13659

Corrigan, A. L., Hanley, S. W., and De Haan, D. O.: Uptake of glyoxal by organic and inorganic aerosol, Environ. Sci. Technol., 42, 4428–4433, doi:10.1021/es7032394, 2008. 13659

Dillon, M. B., Lamanna, M. S., Schade, G. W., Goldstein, A. H., and Cohen, R. C.: Chemical evolution of the Sacramento urban plume: transport and oxidation, J. Geophys. Res., 107(D5), 4045, doi:10.1029/2001JD000969, 2002. 13661

Modeling of glyoxal
at a rural site

A. J. Huisman et al.

Title Page

| Abstract | Introduction |
| Conclusions | References |
| Tables | Figures |

|◄   ►|

◄   ►

Back   Close

Full Screen / Esc

Printer-friendly Version

Interactive Discussion

Edney, E. O., Kleindienst, T. E., Jaoui, M., Lewandowski, M., Offenberg, J. H., Wang, W., and Claeys, M.: Formation of 2-methyl tetrols and 2-methylglyceric acid in secondary organic aerosol from laboratory irradiated isoprene/$NO_x$/$SO_2$/air mixtures and their detection in ambient $PM_{2.5}$ samples collected in the Eastern United States, Atmos. Environ., 39, 5281–5289, doi:10.1016/j.atmosenv.2005.05.031, 2005. 13659

Ervens, B. and Volkamer, R.: Glyoxal processing by aerosol multiphase chemistry: towards a kinetic modeling framework of secondary organic aerosol formation in aqueous particles, Atmos. Chem. Phys., 10, 8219–8244, doi:10.5194/acp-10-8219-2010, 2010. 13660

Fu, T.-M., Jacob, D. J., Wittrock, F., Burrows, J. P., Vrekoussis, M., and Henze, D. K.: Global budgets of atmospheric glyoxal and methylglyoxal, and implications for formation of secondary organic aerosols, J. Geophys. Res., 113, D15303, doi:doi:10.1029/2007JD009505, 2008. 13660

Galloway, M. M., Chhabra, P. S., Chan, A. W. H., Surratt, J. D., Flagan, R. C., Seinfeld, J. H., and Keutsch, F. N.: Glyoxal uptake on ammonium sulphate seed aerosol: reaction products and reversibility of uptake under dark and irradiated conditions, Atmos. Chem. Phys., 9, 3331–3345, doi:10.5194/acp-9-3331-2009, 2009. 13659

Galloway, M. M., Huisman, A. J., Yee, L. D., Chan, A. W. H., Loza, C. L., Seinfeld, J. H., and Keutsch, F. N.: Yields of oxidized volatile organic compounds during the OH radical initiated oxidation of isoprene, methyl vinyl ketone, and methacrolein under high–$NO_x$ conditions, Atmos. Chem. Phys. Discuss., 11, 10693–10720, doi:10.5194/acpd-11-10693-2011, 2011. 13666, 13668

Goldstein, A. H. and Galbally, I. E.: Known and unexplored organic constituents in the Earth's atmosphere, Environ. Sci. Technol., 41, 1514–1521, doi:10.1021/es072476p, 2007. 13658

Goldstein, A. H., Hultman, N. E., Fracheboud, J. M., Bauer, M. R., Panek, J. A., Xu, M., Qi, Y., Guenther, A. B., and Baugh, W.: Effects of climate variability on the carbon dioxide, water, and sensible heat fluxes above a ponderosa pine plantation in the Sierra Nevada (CA), Agr. Forest Meteorol., 101, 113–129, doi:10.1016/S0168-1923(99)00168-9, 2000. 13661

de Gouw, J. A., Middlebrook, A. M., Warneke, C., Goldan, P. D., Kuster, W. C., Roberts, J. M., Fehsenfeld, F. C., Worsnop, D. R., Canagaratna, M. R., Pszenny, A. A. P., Keene, W. C., Marchewka, M., Bertman, S. B., and Bates, T. S.: Budget of organic carbon in a polluted atmosphere: results from the New England Air Quality Study in 2002, J. Geophys. Res., 110, D16305, doi:10.1029/2004JD005623, 2005. 13658

Guenther, A., Geron, C., Pierce, T., Lamb, B., Harley, P., and Fall, R.: Natural emissions of non-

Title Page

| Abstract | Introduction |
| Conclusions | References |
| Tables | Figures |

◄◄ ►►

◄ ►

Back | Close

Full Screen / Esc

Printer-friendly Version

Interactive Discussion

methane volatile organic compounds, carbon monoxide, and oxides of nitrogen from North America, Atmos. Environ., 34, 2205–2230, 2000. 13658

Guenther, A. B., Monson, R. K., and Fall, R.: Isoprene and monoterpene emission rate variability: observations with eucalyptus and emission rate algorithm development, J. Geophys. Res., 96, 10799–10808, 1991. 13663

Hallquist, M., Wenger, J. C., Baltensperger, U., Rudich, Y., Simpson, D., Claeys, M., Dommen, J., Donahue, N. M., George, C., Goldstein, A. H., Hamilton, J. F., Herrmann, H., Hoffmann, T., Iinuma, Y., Jang, M., Jenkin, M. E., Jimenez, J. L., Kiendler-Scharr, A., Maenhaut, W., McFiggans, G., Mentel, Th. F., Monod, A., Prévôt, A. S. H., Seinfeld, J. H., Surratt, J. D., Szmigielski, R., and Wildt, J.: The formation, properties and impact of secondary organic aerosol: current and emerging issues, Atmos. Chem. Phys., 9, 5155–5236, doi:10.5194/acp-9-5155-2009, 2009. 13658

Herndon, S. C., Onasch, T. B., Wood, E. C., Kroll, J. H., Canagaratna, M. R., Jayne, J. T., Zavala, M. A., Knighton, W. B., Mazzoleni, C., Dubey, M. K., Ulbrich, I. M., Jimenez, J. L., Seila, R., de Gouw, J. A., de Foy, B., Fast, J., Molina, L. T., Kolb, C. E., and Worsnop, D. R.: Correlation of secondary organic aerosol with odd oxygen in Mexico City, Geophys. Res. Lett., 35, L15804, doi:10.1029/2008GL034058, 2008. 13658

Hofzumahaus, A., Rohrer, F., Lu, K., Bohn, B., Brauers, T., Chang, C.-C., Fuchs, H., Holland, F., Kita, K., Kondo, Y., Li, X., Lou, S., Shao, M., Zeng, L., Wahner, A., and Zhang, Y.: Amplified trace gas removal in the troposphere, Science, 324, 1702–1704, 2009. 13659

Holzinger, R., Lee, A., Paw, K. T., and Goldstein, U. A. H.: Observations of oxidation products above a forest imply biogenic emissions of very reactive compounds, Atmos. Chem. Phys., 5, 67–75, doi:10.5194/acp-5-67-2005, 2005. 13660

Huisman, A. J., Hottle, J. R., Coens, K. L., Digangi, J. P., Galloway, M. M., Kammrath, A., and Keutsch, F. N.: Laser-induced phosphorescence for the in situ detection of glyoxal at part per trillion mixing ratios, Anal. Chem., 80, 5884–5891, 2008. 13660, 13661, 13662

Intergovernmental Panel on Climate Change: Fourth Assessment Report: Climate Change 2007: Working Group I Report: The Physical Science Basis, Geneva: IPCC, available at: http://www.ipcc.ch/ipccreports/ar4-wg1.htm,last access: 3 May 2011, 2007. 13657

Jakab, G. J., Spannhake, E. W., Canning, B. J., Kleeberger, S. R., and Gilmour, M. I.: The effects of ozone on immune function, Environ. Health Perspect., 103(2), 77–89, doi:, 1995. 13657

Jenkin, M. E., Saunders, S. M., and Pilling, M. J.: The tropospheric degradation of volatile

organic compounds: a protocol for mechanism development, Atmos. Environ., 31, 81–104, doi:10.1016/S1352-2310(96)00105-7, 1997. 13665

Karl, T., Harley, P., Emmons, L., Thornton, B., Guenther, A., Basu, C., Turnipseed, A., and Jardine, K.: Efficient atmospheric cleansing of oxidized organic trace gases by vegetation, Science, 330, 816–819, 2010. 13668

Karnosky, D. F., Gagnon, Z. E., Dickson, R. E., Coleman, M. D., Lee, E. H., and Isebrands, J. G.: Changes in growth, leaf abscission, and biomass associated with seasonal tropospheric ozone exposures of *Populus tremuloides* clones and seedlings, Can. J. For. Res., 26, 23–37, doi:10.1139/x26-003, 1996. 13658

Kroll, J. H. and Seinfeld, J. H.: Chemistry of secondary organic aerosol: formation and evolution of low-volatility organics in the atmosphere, Atmos. Environ., 42, 3593–3624, 2008. 13658

LaFranchi, B. W., Wolfe, G. M., Thornton, J. A., Harrold, S. A., Browne, E. C., Min, K. E., Wooldridge, P. J., Gilman, J. B., Kuster, W. C., Goldan, P. D., de Gouw, J. A., McKay, M., Goldstein, A. H., Ren, X., Mao, J., and Cohen, R. C.: Closing the peroxy acetyl nitrate budget: observations of acyl peroxy nitrates (PAN, PPN, and MPAN) during BEARPEX 2007, Atmos. Chem. Phys., 9, 7623–7641, doi:10.5194/acp-9-7623-2009, 2009. 13670

Lamanna, M. S. and Goldstein, A. H.: In situ measurements of $C_2–C_{10}$ volatile organic compounds above a Sierra Nevada ponderosa pine plantation, J. Geophys. Res., 104(D17), 21247–21262, 1999. 13660, 13661

Lee, A., Goldstein, A. H., Kroll, J. H., Ng, N. L., Varutbangkul, V., Flagan, R. C., and Seinfeld, J. H.: Gas-phase products and secondary aerosol yields from the photooxidation of 16 different terpenes, J. Geophys. Res., 111, D17305, doi:10.5194/10.1029/2006JD007050, 2006. 13666

Lelieveld, J., Butler, T. M., Crowley, J. N., Dillon, T. J., Fischer, H., Ganzeveld, L., Harder, H., Lawrence, M. G., Martinez, M., Taraborrelli, D., and Williams, J.: Atmospheric oxidation capacity sustained by a tropical forest, Nature, 452, 737–740, 2008. 13659

Madronich, S. and Calvert, J. G.: Permutation reactions of organic peroxy radicals in the troposphere, J. Geophys. Res., 95(D5), 5697–5715, 1990. 13658

Murphy, J. G., Day, D. A., Cleary, P. A., Wooldridge, P. J., Millet, D. B., Goldstein, A. H., and Cohen, R. C.: The weekend effect within and downwind of Sacramento – Part 1: Observations of ozone, nitrogen oxides, and VOC reactivity, Atmos. Chem. Phys., 7, 5327–5339, doi:10.5194/acp-7-5327-2007, 2007. 13661

Myriokefalitakis, S., Vrekoussis, M., Tsigaridis, K., Wittrock, F., Richter, A., Brhl, C., Volka-

**Modeling of glyoxal at a rural site**

A. J. Huisman et al.

mer, R., Burrows, J. P., and Kanakidou, M.: The influence of natural and anthropogenic secondary sources on the glyoxal global distribution, Atmos. Chem. Phys., 8, 4965–4981, doi:10.5194/acp-8-4965-2008, 2008. 13660

Nozière, B., Dziedzic, P., and Córdova, A.: Products and kinetics of the liquid-phase reaction of glyoxal catalyzed by ammonium ions ($NH_4^+$), J. Phys. Chem. A, 113, 231–237, 2008. 13659

Orlando, J. J., Tyndall, G. S., Bertman, S. B., Chen, W., and Burkholder, J. B.: Rate coefficient for the reaction of OH with $CH_2{=}C(CH_3)C(O)OONO_2$ (MPAN), Atmos. Environ., 36, 1895–1900, 2002. 13666

Paulot, F., Crounse, J. D., Kjaergaard, H. G., Kurten, A., St. Clair, J. M., Seinfeld, J. H., and Wennberg, P. O.: Unexpected epoxide formation in the gas-phase photooxidation of isoprene, Science, 325, 730–733, doi:10.1126/science.1172910, 2009. 13659

Peeters, J. and Muller, J. F.: $HO_x$ radical regeneration in isoprene oxidation via peroxy radical isomerisations. II: Experimental evidence and global impact, Phys. Chem. Chem. Phys., 12, 14227–14235, 2010. 13659

Peeters, J., Nguyen, T. L., and Vereecken, L.: $HO_x$ radical regeneration in the oxidation of isoprene, Phys. Chem. Chem. Phys., 11, 5935–5939, 2009. 13659

Percy, K. E., Awmack, C. S., Lindroth, R. L., Kubiske, M. E., Kopper, B. J., Isebrands, J. G., Pregitzer, K. S., Hendrey, G. R., Dickson, R. E., Zak, D. R., Oksanen, E., Sober, J., Harrington, R., and Karnosky, D. F.: Altered performance of forest pests under atmospheres enriched by $CO_2$ and $O_3$, Nature, 420, 403–407, doi:10.1038/nature01028, 2002. 13658

Pérez, I. M., LaFranchi, B. W., and Cohen, R. C.: Nitrogen oxide chemistry in an urban plume: investigation of the chemistry of peroxy and multifunctional organic nitrates with a Lagrangian model, Atmos. Chem. Phys. Discuss., 9, 27099–27165, doi:10.5194/acpd-9-27099-2009, 2009. 13666, 13667

Plummer, D. A., McConnell, J. C., Shepson, P. B., Hastie, D. R., and Niki, H.: Modeling of ozone formation at a rural site in Southern Ontario, Atmos. Environ., 30, 2195–2217, 1996. 13658

Ren, X., Olson, J. R., Crawford, J. H., Brune, W. H., Mao, J., Long, R. B., Chen, Z., Chen, G., Avery, M. A., Sachse, G. W., Barrick, J. D., Diskin, G. S., Huey, L. G., Fried, A., Cohen, R. C., Heikes, B., Wennberg, P. O., Singh, H. B., Blake, D. R., and Shetter, R. E.: $HO_x$ chemistry during INTEX–A 2004: Observation, model calculation, and comparison with previous studies, J. Geophys. Res., 113, D05310, doi:10.1029/2007JD009166, 2008. 13659

Saunders, S. M., Jenkin, M. E., Derwent, R. G., and Pilling, M. J.: Protocol for the development of the Master Chemical Mechanism, MCM v3 (Part A): tropospheric degradation of non-

**Modeling of glyoxal at a rural site**

A. J. Huisman et al.

Title Page

| Abstract | Introduction |
| Conclusions | References |
| Tables | Figures |

◄◄   ►►

◄   ►

Back   Close

Full Screen / Esc

Printer-friendly Version

Interactive Discussion

aromatic volatile organic compounds, Atmos. Chem. Phys., 3, 161–180, doi:10.5194/acp-3-161-2003, 2003. 13665

Schade, G. W., Goldstein, A. H., Gray, D. W., and Lerdau, M. T.: Canopy and leaf level 2-methyl-3-buten-2-ol fluxes from a ponderosa pine plantation, Atmos. Environ., 34, 3535–3544, doi:10.1016/S1352-2310(00)00120-5, 2000. 13663

Schlosser, E., Brauers, T., Dorn, H.-P., Fuchs, H., Häseler, R., Hofzumahaus, A., Holland, F., Wahner, A., Kanaya, Y., Kajii, Y., Miyamoto, K., Nishida, S., Watanabe, K., Yoshino, A., Kubistin, D., Martinez, M., Rudolf, M., Harder, H., Berresheim, H., Elste, T., Plass-Dülmer, C., Stange, G., and Schurath, U.: Technical Note: Formal blind intercomparison of OH measurements: results from the international campaign HOxComp, Atmos. Chem. Phys., 9, 7923–7948, doi:10.5194/acp-9-7923-2009, 2009. 13659

Shapiro, E. L., Szprengiel, J., Sareen, N., Jen, C. N., Giordano, M. R., and McNeill, V. F.: Light-absorbing secondary organic material formed by glyoxal in aqueous aerosol mimics, Atmos. Chem. Phys., 9, 2289–2300, doi:10.5194/acp-9-2289-2009, 2009. 13660

da Silva, G.: Hydroxyl radical regeneration in the photochemical oxidation of glyoxal: kinetics and mechanism of the $HC(O)CO + O_2$ reaction, Phys. Chem. Chem. Phys., 12, 6698–6705, 2010. 13659

Spaulding, R. S., Schade, G. W., Goldstein, A. H., and Charles, M. J.: Characterization of secondary atmospheric photooxidation products: evidence for biogenic and anthropogenic sources, J. Geophys. Res., 108, 4247, doi:10.1029/2002JD002478, 2003. 13664

Stavrakou, T., Müller, J.-F., De Smedt, I., Van Roozendael, M., Kanakidou, M., Vrekoussis, M., Wittrock, F., Richter, A., and Burrows, J. P.: The continental source of glyoxal estimated by the synergistic use of spaceborne measurements and inverse modelling, Atmos. Chem. Phys., 9, 8431–8446, doi:10.5194/acp-9-8431-2009, 2009. 13660

Stavrakou, T., Peeters, J., and Müller, J.-F.: Improved global modelling of $HO_x$ recycling in isoprene oxidation: evaluation against the GABRIEL and INTEX-A aircraft campaign measurements, Atmos. Chem. Phys., 10, 9863–9878, doi:10.5194/acp-10-9863-2010, 2010. 13659

Steiner, A. L., Tonse, S., Cohen, R. C., Goldstein, A. H., and Harley, R. A.: Biogenic 2-methyl-3-buten-2-ol increases regional ozone and $HO_x$ sources, Geophys. Res. Lett., 34, L15806, doi:10.1029/2007GL030802, 2007. 13671

Steiner, A. L., Cohen, R. C., Harley, R. A., Tonse, S., Millet, D. B., Schade, G. W., and Goldstein, A. H.: VOC reactivity in central California: comparing an air quality model to ground-based measurements, Atmos. Chem. Phys., 8, 351–368, doi:10.5194/acp-8-351-

Title Page

Abstract | Introduction

Conclusions | References

Tables | Figures

◄ | ►

◄ | ►

Back | Close

Full Screen / Esc

Printer-friendly Version

Interactive Discussion

2008, 2008. 13658

Sumner, A. L., Shepson, P. B., Couch, T. L., Thornberry, T., Carroll, M. A., Sillman, S., Pippin, M., Bertman, S., Tan, D., Faloona, I., Brune, W., Young, V., Cooper, O., Moody, J., and Stockwell, W.: A study of formaldehyde chemistry above a forest canopy, J. Geophys. Res., 106(D20), 24387–24405, 2001. 13665

Tan, D., Faloona, I., Simpas, J. B., Brune, W., Shepson, P. B., Couch, T. L., Sumner, A. L., Carroll, M. A., Thornberry, T., Apel, E., Riemer, D., and Stockwell, W.: HO$_x$ budgets in a deciduous forest: Results from the PROPHET summer 1998 campaign, J. Geophys. Res., 106(D20), 24407–24427, 2001. 13659

Tan, Y., Perri, M. J., Seitzinger, S. P., and Turpin, B. J.: Effects of precursor concentration and acidic sulfate in aqueous glyoxal-OH radical oxidation and implications for secondary organic aerosol, Environ. Sci. Technol., 43, 8105–8112, 2009. 13660

Taraborrelli, D., Lawrence, M. G., Butler, T. M., Sander, R., and Lelieveld, J.: Mainz Isoprene Mechanism 2 (MIM2): an isoprene oxidation mechanism for regional and global atmospheric modelling, Atmos. Chem. Phys., 9, 2751–2777, doi:10.5194/acp-9-2751-2009, 2009. 13658

Thornton, J. A., Wooldridge, P. J., Cohen, R. C., Martinez, M., Harder, H., Brune, W. H., Williams, E. J., Roberts, J. M., Fehsenfeld, F. C., Hall, S. R., Shetter, R. E., Wert, B. P., and Fried, A.: Ozone production rates as a function of NO$_x$ abundances and HO$_x$ production rates in the Nashville urban plume, J. Geophys. Res., 107, doi:10.1029/2001JC001083, 2002. 13659

Trainer, M., Williams, E. J., Parrish, D. D., Buhr, M. P., Allwine, E. J., Westberg, H. H., Fehsenfeld, F. C., and Liu, S. C.: Models and observations of the impact of natural hydrocarbons on rural ozone, Nature, 329, 705–707, doi:10.1038/329705a0, 1987. 13658

Volkamer, R., Jimenez, J. L., San Martini, F., Dzepina, K., Zhang, Q., Salcedo, D., Molina, L. T., Worsnop, D. R., and Molina, M. J.: Secondary organic aerosol formation from anthropogenic air pollution: rapid and higher than expected, Geophys. Res. Lett., 33, L17811, doi:10.1029/2006GL026899, 2006. 13658

Volkamer, R., San Martini, F., Molina, L. T., Salcedo, D., Jimenez, J. L., and Molina, M. J.: A missing sink for gas-phase glyoxal in Mexico City: formation of secondary organic aerosol, Geophys. Res. Lett., 34, L19807, doi:10.1029/2007GL030752, 2007. 13659, 13660, 13665, 13666, 13669

Volkamer, R., Ziemann, P. J., and Molina, M. J.: Secondary Organic Aerosol Formation from Acetylene (C$_2$H$_2$): seed effect on SOA yields due to organic photochemistry in the aerosol

aqueous phase, Atmos. Chem. Phys., 9, 1907–1928, doi:10.5194/acp-9-1907-2009, 2009. 13669

Whalley, L. K., Edwards, P. M., Furneaux, K. L., Goddard, A., Ingham, T., Evans, M. J., Stone, D., Hopkins, J. R., Jones, C. E., Karunaharan, A., Lee, J. D., Lewis, A. C., Monks, P. S., Moller, S. J., and Heard, D. E.: Quantifying the magnitude of a missing hydroxyl radical source in a tropical rainforest, Atmos. Chem. Phys. Discuss., 11, 5785–5809, doi:10.5194/acpd-11-5785-2011, 2011. 13659

Wolfe, G. M., Thornton, J. A., Yatavelli, R. L. N., McKay, M., Goldstein, A. H., LaFranchi, B., Min, K.-E., and Cohen, R. C.: Eddy covariance fluxes of acyl peroxy nitrates (PAN, PPN and MPAN) above a Ponderosa pine forest, Atmos. Chem. Phys., 9, 615–634, doi:10.5194/acp-9-615-2009, 2009. 13661

Wolfe, G. M., Thornton, J. A., Bouvier-Brown, N. C., Goldstein, A. H., Park, J.-H., McKay, M., Matross, D. M., Mao, J., Brune, W. H., LaFranchi, B. W., Browne, E. C., Min, K.-E., Wooldridge, P. J., Cohen, R. C., Crounse, J. D., Faloona, I. C., Gilman, J. B., Kuster, W. C., de Gouw, J. A., Huisman, A., and Keutsch, F. N.: The Chemistry of Atmosphere-Forest Exchange (CAFE) Model – Part 2: Application to BEARPEX-2007 observations, Atmos. Chem. Phys., 11, 1269–1294, doi:10.5194/acp-11-1269-2011, 2011. 13659

Wood, E. C., Canagaratna, M. R., Herndon, S. C., Onasch, T. B., Kolb, C. E., Worsnop, D. R., Kroll, J. H., Knighton, W. B., Seila, R., Zavala, M., Molina, L. T., DeCarlo, P. F., Jimenez, J. L., Weinheimer, A. J., Knapp, D. J., Jobson, B. T., Stutz, J., Kuster, W. C., and Williams, E. J.: Investigation of the correlation between odd oxygen and secondary organic aerosol in Mexico City and Houston, Atmos. Chem. Phys., 10, 8947–8968, doi:10.5194/acp-10-8947-2010, 2010. 13658

Zhang, Q., Jimenez, J. L., Canagaratna, M. R., Allan, J. D., Coe, H., Ulbrich, I., Alfarra, M. R., Takami, A., Middlebrook, A. M., Sun, Y. L., Dzepina, K., Dunlea, E., Docherty, K. S., DeCarlo, P. F., Salcedo, D., Onasch, T., Jayne, J. T., Miyoshi, T., Shimono, A., Hatakeyama, S., Takegawa, N., Kondo, Y., Schneider, J., Drewnick, F., Borrmann, S., Weimer, S., Demerjian, K., Williams, P., Bower, K., Bahreini, R., Cottrell, L., Griffin, R. J., Rautiainen, J., Sun, J. Y., Zhang, Y. M., and Worsnop, D. R.: Ubiquity and dominance of oxygenated species in organic aerosols in anthropogenically-influenced Northern Hemisphere midlatitudes, Geophys. Res. Lett., 34, L13801, doi:10.1029/2007GL029979, 2007. 13658

A. J. Huisman et al.

Title Page

Abstract | Introduction

Conclusions | References

Tables | Figures

◀ | ▶

◀ | ▶

Back | Close

Full Screen / Esc

Printer-friendly Version

Interactive Discussion

**Table 1.** Glyoxal dataset parameters by temperature period, all values in $\text{ppt}_v$.

| Period | Mean | 95% bounds | |
|---|---|---|---|
| | | Lower | Upper |
| Campaign | 43.6 | 4.6 | 121.7 |
| Hot | 53.9 | 22.3 | 127.3 |
| Cold | 16.3 | 0.9 | 48.4 |
| Intermediate | 42.1 | 19.4 | 93.4 |
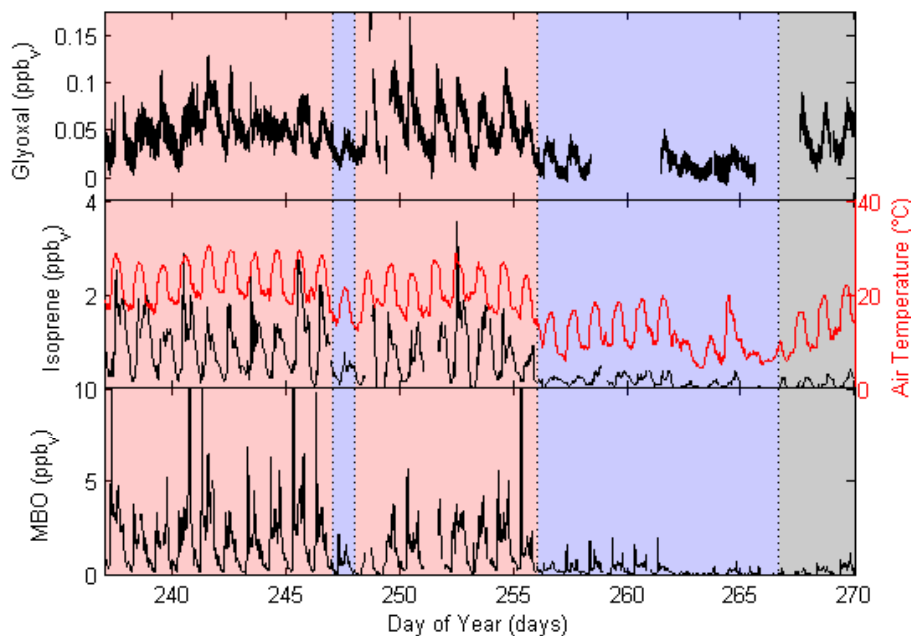
**Fig. 1.** Overview of glyoxal measurements, separated by temperature period (red, blue, gray corresponding to hot, cold, and intermediate period). Isoprene and MBO, the most important glyoxal BVOC precursors, are included along with air temperature on the center axis on right.
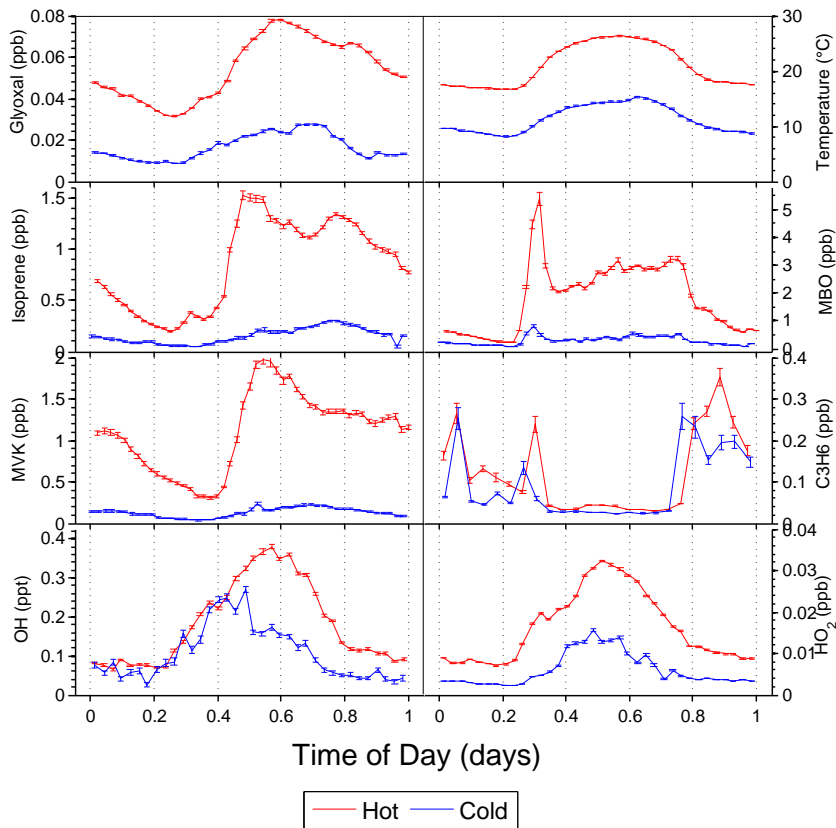
**Fig. 2.** Diurnal averages of glyoxal, temperature, example biogenic and anthropogenic species, and HO$_x$ separated into hot, and cold period. Here the hot period spans 15 d. The cold period contains only data for which glyoxal was recorded. Error bars indicate the 1 standard deviation envelope as calculated based on the variability in the data from day to day and neglecting reported or calculated error from each measurement.
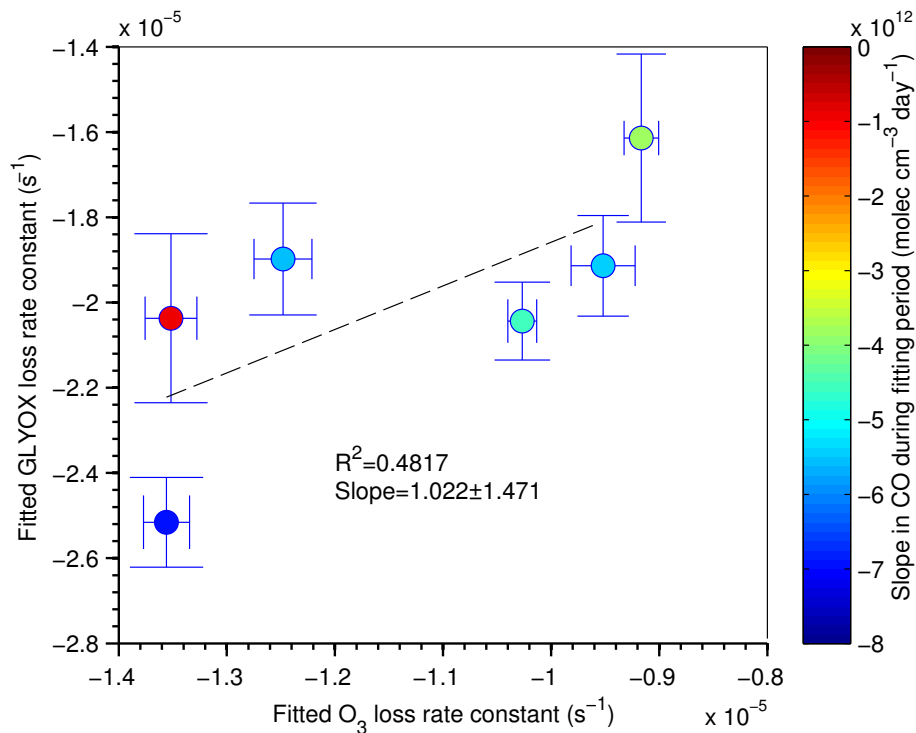
**Fig. 3.** Fitted deposition rates for glyoxal and $O_3$ from data taken at BEARPEX 2007. Color coding of points indicates the slope in CO, and indicator of the stability or dilution of the airmass.
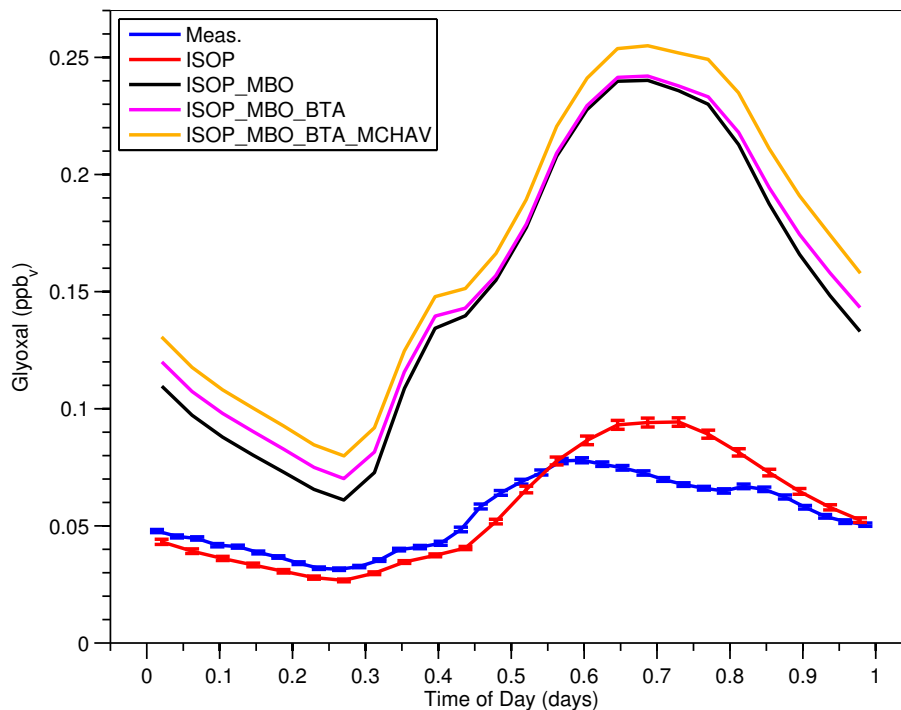
**Fig. 4.** Diurnally averaged model results from the hot period showing the incremental contributions of various VOC precursors. The model VOC precursor subsets correspond to: ISOP = isoprene; MBO = MBO; BTA = benzene, toluene, acetylene, and pinenes; MCHAV = methylchavicol. Error bars are omitted from upper traces for clarity, all are approximately equal in magnitude to those shown for that of ISOP.
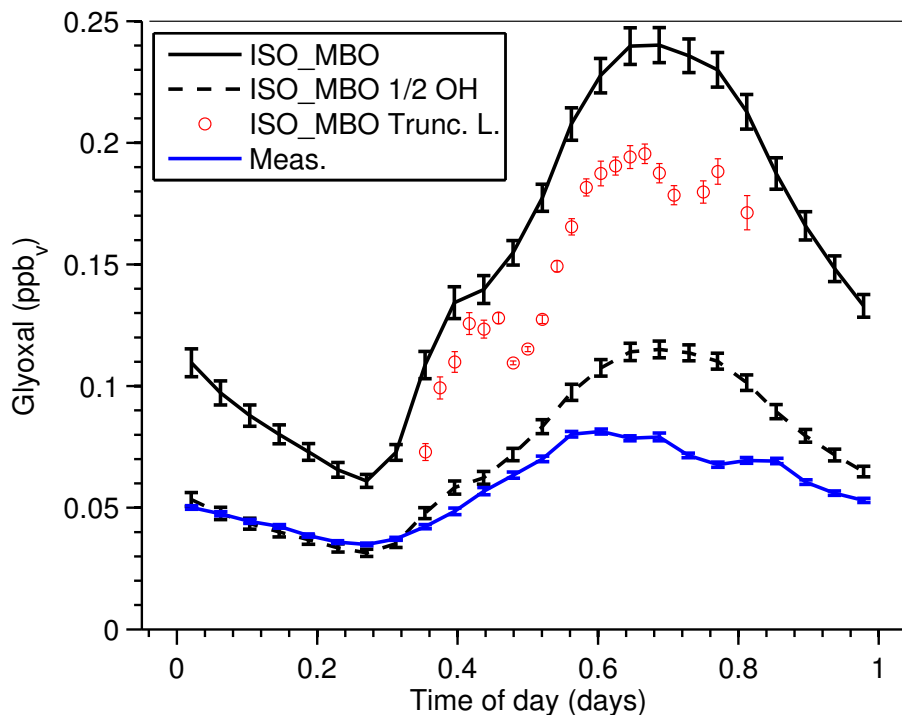
**Fig. 5.** Model results for OH sensitivity study. Simulations were performed using ambient OH and 1/2 OH using combined isoprene and MBO chemistry. The Truncated Lagrangian model (daytime only) is shown for comparison. Error bars indicate the 1 standard deviation envelope as calculated based on the variability in the data and model outputs, not reported errors.
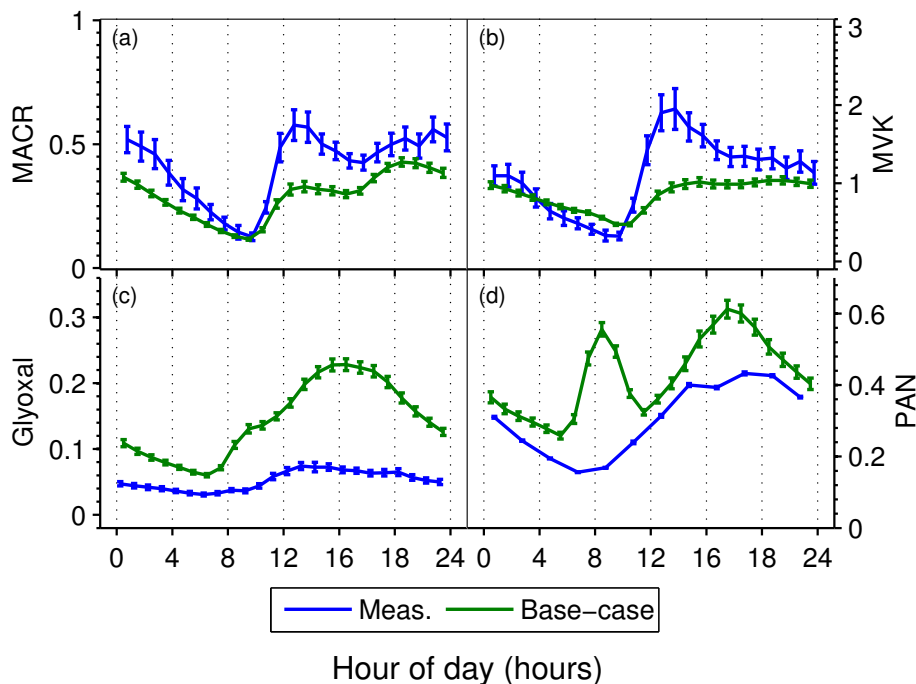
**Fig. 6.** Summary of model OVOCs and measurements as available, all in ppb. The model is broadly able to predict MVK and MACR, while it exceeds measurements of glyoxal substantially. The slight under-prediction of MVK and MACR is expected for the 0-D-box model as it underestimates the contribution of isoprene oxidation, which is largely emitted upwind of the measurement site. Error bars indicate the 1 standard deviation envelope as calculated based on the variability in the data, not reported errors.